

Raman spectroscopy and low temperature electrical conductivity study of thermally evaporated CdS thin films

Rashmitha Keshav¹ · Ashok Rao¹ · M. G. Mahesha¹

Received: 30 October 2017 / Accepted: 27 March 2018 / Published online: 30 March 2018
© Springer Science+Business Media, LLC, part of Springer Nature 2018

Abstract A systematic study has been carried out on properties of CdS thin films grown on glass substrates by thermal route and growth parameters have been optimized to achieve near stoichiometry. Raman spectroscopy of the films has been carried out to get more insight on chemical and structural information of the films. Photoluminescence study was carried out to get the knowledge of defect-states which play major role in transport mechanisms. In order to obtain electrical parameters, Hall measurement has been carried out by van der Pauw's technique at room temperature. Also, variation of electrical resistivity of the films at temperature range 20–300 K has been studied. Finally effect of post deposition annealing on the structural, optical and electrical properties of these films has been studied.

Keywords X-ray diffraction · Physical vapor deposition processes · Raman spectroscopy · Low temperature conductivity · Semiconducting cadmium compounds

1 Introduction

In the recent past, there has been an increase in research and development of the IIB—VIA compound semiconductors because of their importance as prospective members in scientific, technological and industrial applications in optoelectronics particularly solar cells (Ullrich et al. 2000; Britt and Ferekides 1993). Short optical absorption length and difficulty of forming a shallow junction with a high-conductivity surface layer are main reasons due to which solar cells made up of polycrystalline thin-film normally have hetero-junction configuration. Due to favourable reasons like intermediate band gap, stability and high absorption coefficient, CdS is the material of intense research in the thin film form. As-deposited n type-CdS with a relatively wide band gap (~2.4 eV) was found to be best fitted as the hetero-junction partner or 'window' for thin-film solar cells based on CdTe,

✉ M. G. Mahesha
mahesham@gmail.com

¹ Department of Physics, Manipal Institute of Technology, Manipal University, Manipal 576104, India

which is most assuring thin-film photovoltaic material (Chu et al. 1992; Wu et al. 2001). Optimization of thickness of CdS films is very essential to achieve high optical transmission and uniformity with the assurance of no electrical short-circuit effects (Oliva et al. 2003). It is the established fact that preparation techniques and parameters highly influence the electrical and optical properties of the films. Among the various deposition techniques available, vacuum evaporation (VE) is known to be trouble-free and controllable technique for large-area deposition. Even though CdS has been studied in thin film form by several researchers, there are not many reports on Raman scattering and low temperature electrical conductivity analysis of the films. Raman analysis is a powerful technique which can give detailed structural and chemical information. Hence it is appropriate to adopt the technique to understand the structural and chemical modifications happening during annealing of the film. Also, it is essential to investigate the electrical property to ensure the device suitability of the prepared film. Therefore, the present paper is centred over the study of Raman spectrum and electrical conductivity at low temperature along with associated studies to obtain knowledge on structural and optical properties.

2 Experimental

CdS thin film of 300 nm thickness was deposited by thermal evaporation of stoichiometric powder of the compound (99.99%) in a residual pressure of 10^{-6} Torr. Molybdenum boat sources were used for the evaporation. The deposition rate and thickness were monitored by digital film thickness monitor using a quartz crystal sensor set at 6 MHz (DTM-10). The deposition rate was optimized to 0.3 nm/s. Deposited films have been annealed at various temperatures under air ambience for an hour. The crystal structure of the films was studied by X-ray diffraction (XRD) technique using a Rigaku Miniflex-600 with the radiation source of Cu $K\alpha$ (0.154 nm) at 40 kV, 15 mA in scanning range 20° – 70° at scan speed of $2^{\circ}/\text{min}$. The surface morphology of the films was analysed by scanning electron microscopy (SEM) model Zeiss SEM EVO18 and atomic force microscopy (AFM) model BRUKER INNOVA. The root mean square (RMS) surface roughness was calculated from AFM micrographs. Optical properties of the films were examined by Shimadzu UV-1800 PC spectrophotometer in UV–Vis–NIR wavelengths ranged from 300 to 1100 nm. Raman studies have been done using Thermo Nicolet 670 at 180° geometry with Nd:YAG laser (1064 nm) as source. The photoluminescence study has been carried out using Agilent Cary Eclipse WinFLR photoluminescence spectrometer. Keithley 2450 source meter has been used for electrical characterizations including Hall measurements. Temperature dependent electrical resistivity measurements were carried out for a temperature range of 20–300 K in a closed cycle refrigerator (CCR) using conventional four probe technique.

3 Results and discussion

3.1 Structural and morphological characterization

X-ray diffractograms recorded for as-deposited and annealed CdS thin films were compared. Sharpness and height of the XRD peaks are two important parameters which can be used to assess the crystallite size and degree of crystallinity of the samples. Plot of degree of crystallinity and FWHM for films annealed at various temperatures is depicted in Fig. 1a. Initially

the crystallinity has improved with annealing temperature and then it showed declining trend. Films annealed at 673 K have shown greatest degree of crystallinity and maximum crystallite size. Hence this sample has been selected for further study and compared with the as-deposited films for structural, optical and electrical properties. Typical XRD patterns of as-deposited and annealed CdS films are shown in Fig. 1b, c. Rietveld refinement technique was adopted to analyse XRD data and hence to obtain crystallographic information. Refinement is a process which minimizes the sum of squares of the weighted differences between the observed and calculated intensities for every point in the profile under the Bragg reflections. This is achieved by adjusting structural constants like lattice parameters, thermal parameters, atomic coordinates and profile parameters such as U, V, W and diffractometer zero point (Von Dreele et al. 1982).

For as-deposited films, as it can be seen, the pattern is composed of a dominant peak at 2θ value 26.64° which can be assigned to the plane (111) of CdS cubic phase (JCPDS card no. 10-0454). The films have remained in cubic structure even after annealing, however, peak has shifted to 26.24° with increased intensity. Effect of the uniform lattice strain on the diffraction peak position was observed resulting in peak shift towards lower angles confirmed through lattice constants (Table 1). CdS usually exists in two crystallographic phases namely, wurtzite (α -phase) and zinc blende (β -phase). The latter is a face centred cubic (f.c.c.) structure which may be considered as two interpenetrating face centred lattices of the elements, with the corner of one located at the position $\frac{1}{4}\frac{1}{4}\frac{1}{4}$ of the other, as in the diamond structure. The zinc blende structure is related to the wurtzite structure which has one kind of atom on close packed hexagonal positions and the other at intermediate points, corresponding to tetrahedral voids where each atom is surrounded symmetrically by four atoms of the other kind. The hexagonal layers are stacked in one sequence in wurtzite and in another in zinc-blende. Literature survey shows that transformation temperature for wurtzite-zinc blende is about 1273 K (Boaky and Nusenu 1997) and growth of CdS films at low substrate temperature (<373 K) favours cubic structure even with different preparation techniques like RF sputtering and laser ablation (El Assali et al. 2000; Sakai et al. 1998). The crystallite size of deposited films is estimated by using Debye–Scherrer’s formula (Chandramohan et al. 2008).

$$D = \frac{0.94\lambda}{\beta \cos \theta} \quad (1)$$

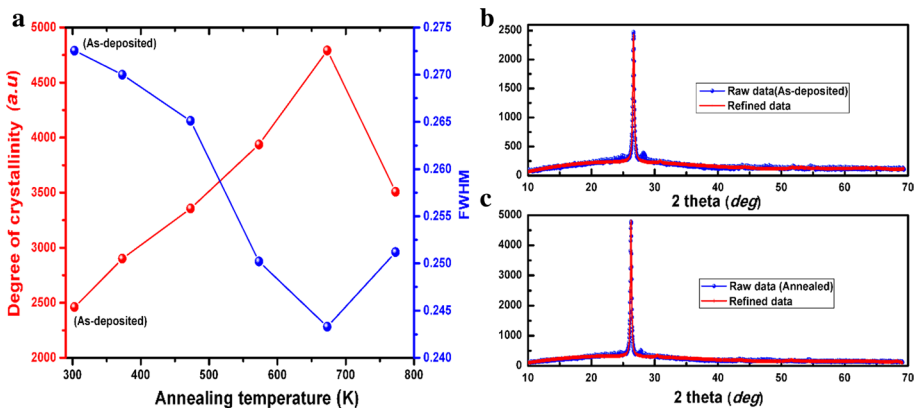


Fig. 1 a Comparison of crystallinity of films annealed at different temperatures. b X-ray diffractogram with refined data for as-deposited and c 673 K annealed films

Table 1 Crystallographic data obtained from refinement of X-ray diffractogram

Sample	2θ	d (nm)	hkl	Atom	x/a	y/b	z/c	a = b = c (nm)	$\alpha = \beta = \gamma$	Cell volume (nm ³)	Strain ($\epsilon \times 10^{-4}$)
As deposited	26.64	0.334	111	Cd	0.0000	0.0000	0.0000	0.579	90°	0.194	11.4
				S	0.2500	0.2500	0.2500				
Annealed	26.24	0.339	111	Cd	0.0000	0.0000	0.0000	0.587	90°	0.203	10.2
				S	0.2500	0.2500	0.2500				

where θ is diffraction angle of the concern diffraction peak, λ is wavelength of radiation used, β is FWHM of the diffraction peak. Calculated crystallite size is found to be 31 nm for as-deposited and 35 nm for annealed films. Comparatively smaller crystallite size in the as-deposited film can be attributed to relatively low substrate temperature where condensation and sticking to the region of hit of ad-atoms is more probable compared to migration towards neighbouring crystallite. The increase of crystallite size in annealed film may be attributed to coalesce of the smaller crystallites into effectively larger crystallites. Strain $\epsilon = \frac{\beta \cos \theta}{4}$ in the films has been determined and presented in Table 1. Decreased strain in annealed films reflects decrease in lattice imperfections and an increase in crystallite size.

The SEM examination of microstructure of as-grown and annealed CdS thin films (Fig. 2a, b) reveal that prepared films are homogeneous, crack free, dense and exhibit almost complete coverage on the substrate. Significant morphological changes in heat treated films as compared with as-deposited films is evident from the SEM micrograph. Energy dispersive spectrograph (EDS) proves that the atomic percentage of as-deposited films was nearly stoichiometric (Cd to S ratio 1:0.996, slightly Cd rich) and after annealing, no considerable change was observed in the film composition. In addition, elemental mapping (Fig. 2c, d) confirms that distribution of constituent elements of the compound is homogeneous over considerably large area which is an essential requirement for reliability and repeatability of the performance of the devices fabricated using any deposition technique.

Figure 3 shows AFM micrographs of as-deposited and annealed films recorded over the scanning area of $2 \times 2 \mu\text{m}$ square. Micrographs corresponding to as-grown films exhibit

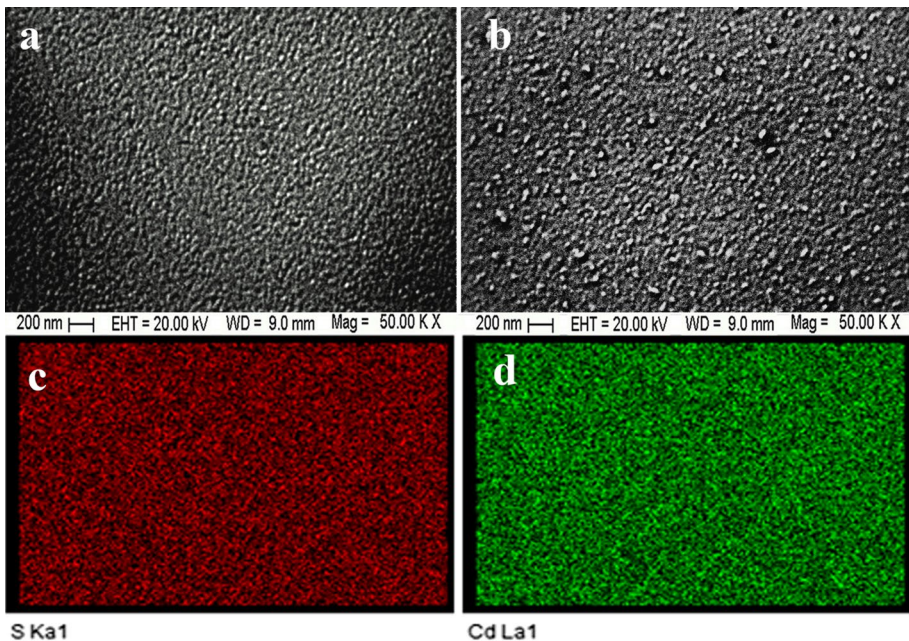


Fig. 2 SEM micrographs of CdS films of 300 nm before and after heat treatment: **a** As-deposited film; **b** Film annealed at 673 K; **c** and **d** Compositional maps of compound, S and Cd respectively for as-deposited film

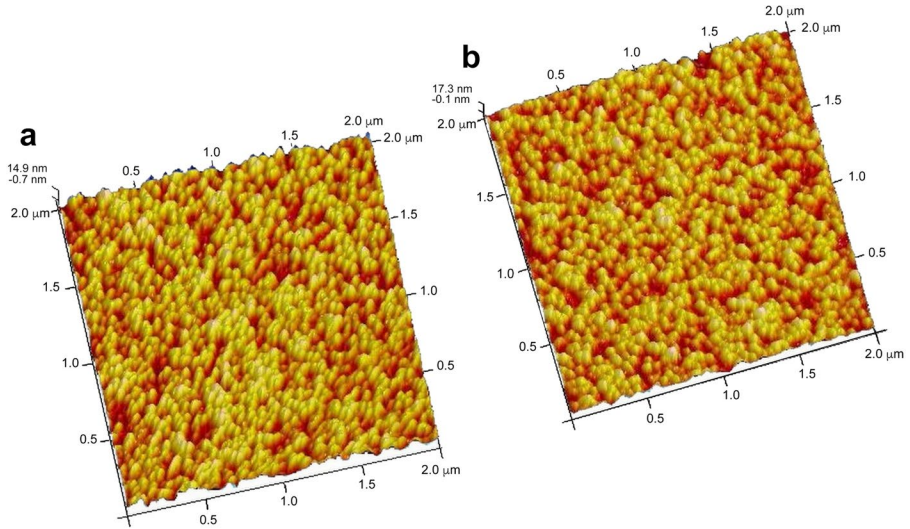


Fig. 3 AFM micrographs of CdS films: **a** As-deposited films. **b** Films annealed at 673 K

growth as columns leaving gap in between the grains (Hasnat and Podder 2012). Annealing resulted larger crystallites with vertical growth. It is an established fact that surface roughness, a direct result of deposition and post deposition process, leads to a considerable impact on surface properties. Estimation of RMS surface roughness, defined as the standard deviation of the surface height profile from the average height, shows that surface roughness increases from 4.60 and 5.01 nm after annealing.

3.2 Optical characterization

Figure 4a represents the optical transmittance spectra recorded for as-deposited and annealed CdS films. Multiple beam interference fringes observed in both the films indicate good degree of uniformity in film thickness. As-deposited films have shown average transmittance of about 84% with sharp band edge at about 505 nm. About 6% reduction

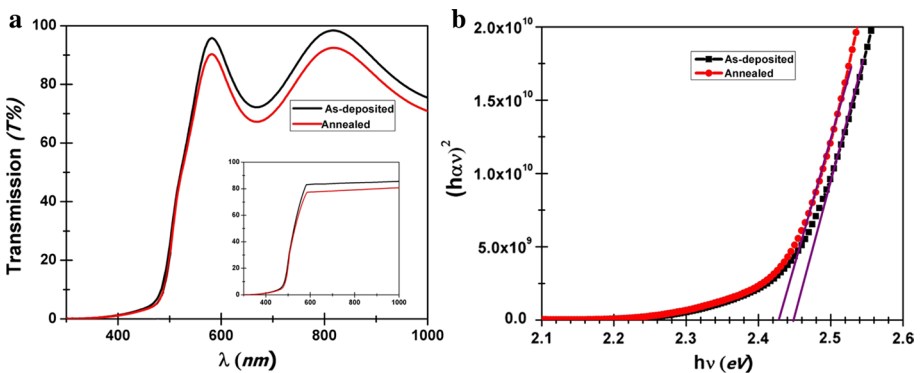


Fig. 4 **a** Recorded transmittance spectra (Inset: PARAV fit) and **b** Plot of $(\alpha h\nu)^2$ versus $h\nu$ for CdS films

in the transmittance has been observed for the annealed films which can be attributed to crystallite size effect and degree of crystallinity (Qinghui et al. 2007). Similar behaviour in the transmission spectra of the CdS films prepared by other techniques have been reported in the literature (Hasnat and Podder 2012). Software tool “PARAV” is used to reassess the average thickness and to calculate optical constants from the transmission spectra. PARAV fitted transmission spectra which negated the interference effect is shown as in-set in Fig. 4a.

The energy band gap of the films was calculated by using Tauc relation (Prabhar and Dhanam 2005).

$$\alpha h\nu = A(E_g - h\nu)^n \quad (2)$$

where A is a constant α is the absorption coefficient, and $h\nu$ is the photon energy. In the case of direct band gap transition ‘ n ’ is taken as $\frac{1}{2}$. The linear part of the $(\alpha h\nu)^2$ versus $h\nu$ plot shown in Fig. 4b describes the direct allowed transition of CdS thin films. The estimated optical band gap is 2.45 eV for as-deposited films and 2.43 eV for films annealed at 673 K. Shift towards bulk value (2.42 eV) in the optical band-gap for annealed film can be endorsed to increased crystallite size or improved crystallinity and release in the strain.

The obtained spectral dependence of the optical constants refractive index (n) and extinction coefficient (k) are illustrated in Fig. 5a, b. Here the refractive index, obtained from ‘PARAV’ which adopted Swanepoel method, has shown increase after annealing treatment. The peak values of the refractive index of the films varied in the range of 2.14–2.28 over the spectral range 600–1100 nm. Better crystallinity in the annealed films or increase in the crystallite size leads to the higher value of n , which in turn increases the optical reflectance and decreases the transmission. The extinction coefficient k of the thin films is also calculated using the formula (Prabhar and Dhanam 2005).

$$k = \frac{\alpha\lambda}{4\pi} \quad (3)$$

k decreases rapidly with increasing wavelength in the range from 400 to 600 nm. In the forbidden energy gap region, variation of the extinction coefficient is dictated by light absorption. In the case of polycrystalline films, non-zero value of k for photon energies smaller

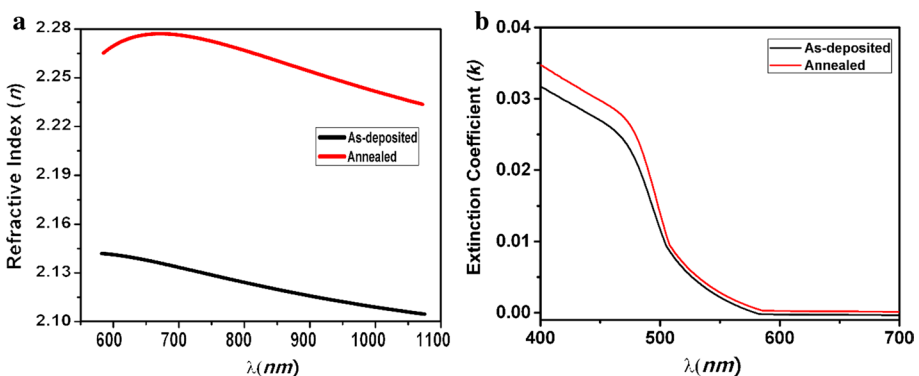


Fig. 5 **a** Variation of n with wavelength. **b** Variation of k with wavelength

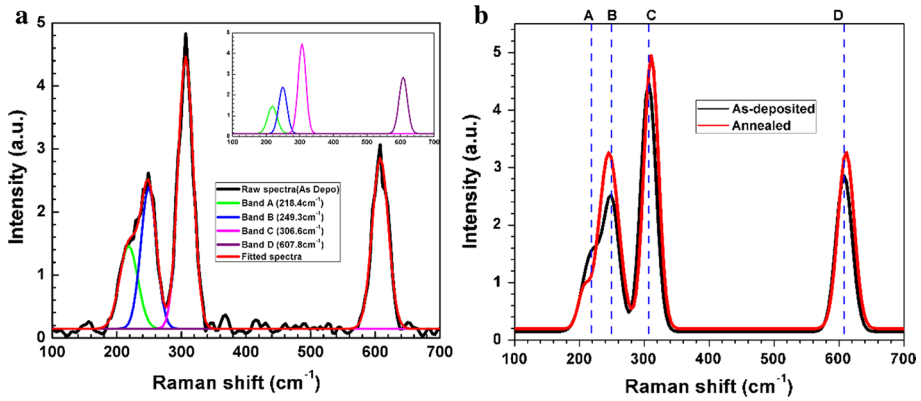


Fig. 6 **a** Raman spectra of as-grown (inset: de-convoluted peaks) and **b** Comparison of Raman spectra of as-grown and annealed CdS thin films (after baseline correction)

Table 2 Comparison of Raman data

Sample	A (cm ⁻¹)	B (cm ⁻¹)	C (cm ⁻¹)	D (cm ⁻¹)
As-grown CdS film	218.4	249.3	306.6	607.8
Annealed CdS film	206.6	245.2	310.7	610.8
Trajić et al. (2015)	212	245	305	611
Chuu et al. (1991)	–	–	296	600
Farid et al. (2012)	–	–	303	608
Lee (2004)	–	–	300	605
Senthil et al. (2001)	–	–	299	–
Tell et al. (1966)	–	–	305	–

than the fundamental absorption edge is generally observed which is due to extra absorption of light at the grain boundaries.

3.3 Raman scattering analysis

Figure 6a depicts Raman spectra of as-grown CdS thin films and Fig. 6b compares Raman spectra of as-grown CdS film with that of annealed film. Four prominent Raman bands have been observed in both the samples. The approximate band positions for as-grown films are as follows: Band A ~218.4 cm⁻¹, band B ~249.3 cm⁻¹, band C ~306.6 cm⁻¹ and band D ~607.8 cm⁻¹. Present work reports the investigation of Raman scattering from phonons propagating on the polycrystalline CdS thin films which may be considered under weak confinement regime according to the literature (Irimpan et al. 2008). Analysis of Raman peaks has engendered considerable debate in the literature (Abdulkhadar and Thomas 1995; Trajić et al. 2015; Chuu et al. 1991; Farid et al. 2012; Lee 2004; Senthil et al. 2001; Tell et al. 1966). Table 2 provides the comparison of Raman study of CdS thin films done by various research groups.

In CdS, the difference in frequency of LO (longitudinal optical phonons) and TO (transverse optical phonons) propagating parallel and perpendicular to the optic axis is roughly

equal to zero, exhibiting negligible optical anisotropy which can be approximated as cubic nature (Abdulkhadar and Thomas 1995). As revealed from detailed analysis of X-ray diffractogram, films have zinc blende crystal structure belonging to F-43 m (216) space group. Trajić et al. (2015) have reported protuberant bands at 212 cm^{-1} with B_2 symmetry, E_1 symmetry mode at 245 cm^{-1} and longitudinal mode at 305 cm^{-1} with its first overtone at 611 cm^{-1} for CdS crystals. In present case, multiphonon lines are shifted by energies which are approximately 1% less than exact multiple of 1LO line i.e. 306.6 cm^{-1} . 2LO is also known as overtone of 1LO observed at 607.8 cm^{-1} . Presence of only two characteristic longitudinal optical phonon peaks of CdS here is due to the laser frequency being less than the gap E_g/h (Leite et al. 1969). FWHM and frequency shift are two important features that can give insight to the crystallinity, purity and induced strain in the hetero-structure. Compared to the spectra of the bulk, in the present study, we observed blue shift in the spectral bands of CdS films. Also, FWHM for 1LO has decreased from 23.19 cm^{-1} (as-grown) to 22.45 cm^{-1} (annealed). Frequency shift may be observed due to several reasons. In the present study, mostly strain effect can be responsible for frequency shift as there is mismatch in the thermal properties of the film and substrate. In case of as-deposited films, higher FWHM can also be resultant of polycrystalline effect which is corroborated by the appearance of XRD pattern. Decrease in FWHM or sharpening of the peak in annealed films can be referred to larger crystallite size which can be further attributed to the increase in surface roughness imputable to the fact that surface occupies most of the total volume of the film. i.e., large number of atoms residing on the surface. Finally release of random strain leading to better crystallinity and allowing minimum energy configuration, can also be the cause of decrement in FWHM of the annealed film. Imperfections and impurities could also give rise to frequency shift. The overall intensities of the peaks of as-deposited CdS film are weaker than those of annealed films. The variations in ratios of intensities as a function of particle size is considered and encountered that, the ratio of I_{2LO}/I_{1LO} increased as the particle size increases which is a measure of strength of the electron-phonon interaction. V. Sivasubramanian et al. also reported increase in the electron-phonon coupling as function of particle size irrespective of structure. (Sivasubramanian et al. 2006).

In case of bulk crystalline semiconducting materials or thicker films ($> 100\text{ }\mu\text{m}$), for the similar excitation wavelength, Raman shifts correspond to the longitudinal optical phonons (LO) and due to symmetry restrictions and low intensity, transverse optic (TO) and the surface phonon (SP) modes are not observable (Filippidis et al. 1999; Badr et al. 2004). But, in nano-structured thin films, due to large surface to volume ratio, SP mode is likely to be observable. In case of nano-structured thin film semiconductors, due to finite size of the particles, charge carriers in conduction and valence bands experience confining potential. It leads to size-dependent discrete states in the conduction and valence bands resulting in effective boost of the band gap. Also excess of Cd results in acceptor states within the gap of CdS which produces localized states near the valence band edge. Furthermore, phonon interaction with these states creates electron-hole pairs due to which self-energy is acquired by the phonon and in turn it shifts the frequency of SP mode to higher values (Nanda et al. 1999).

Relatively weaker band A $\sim 218.4\text{ cm}^{-1}$, band B $\sim 249.3\text{ cm}^{-1}$ can be allotted to TO and SP modes respectively. Modes in Raman are normally size dependent and with size reduction SP mode is likely to observe between LO and TO modes (Kozyskiy et al. 2014; Dzhagan et al. 2016). The present allotment is in close agreement with the results obtained by Chi et al. (2011). This conclusion can be toned by explaining difference between the surface layers and the internal structure of particle and the reliance of surface modes on arrangement of atoms on the surface layers which can be detected in the Raman spectra of

thin films (Abdulkhadar and Thomas 1995). Even though sulphur is highly Raman sensitive, we have not observed any band corresponding to it which confirms that decomposition of CdS during the deposition is negligible.

3.4 Photo-luminescence analysis

Photo-luminescence (PL) is a powerful tool to examine the quality of polycrystalline thin films by determining the radiative active defects which can act as traps in carrier transport. Most of the direct band gap materials possess a general property of emission of light called luminescence and if cause of carrier excitation is photon absorption, radiation resulting from the excited carriers is known to be photoluminescence. CdS thin film can be an appealing host for photonic devices due to its expected gap emission, which is close to the highest sensitivity of human eye. In this work photoluminescence of CdS films were performed in room temperature for excitation wavelength 413 nm. Figure 7a. shows the peaks at 2.22, 2.33 (green emission) and 1.96 eV (red emission). Films exhibited luminescence peak at energies lower when compared to the band gap which assigns the impurities in mid-band gap region. As evidenced in elemental analysis, balanced stoichiometry resulted in red and green band emission regardless of annealing effect (Hwang et al. 2012). Though the peak shift has not been manifested, the enhanced intensity of the bands for smaller crystallite size may be attributed to the larger-surface to volume ratio. Hence CdS thin films with smaller crystallite size demonstrate higher intensity luminescence when compared to the larger crystallite diameter. Here the red band emission can be attributed to the transitions of electrons trapped at surface states to the valence band and green band (2.22 eV) can be assigned donor-acceptor-pair (DAP) recombination of $(\text{Cd}_i-\text{V}_{\text{Cd}}^-)$ Frenkel defect complexes. Origin of second green emission (2.33 eV) can be due to radiative recombination of electrons and holes via surface/defect states present which is associated with transition between the shallow acceptor S_i (sulphur interstitials) and CB or the transition

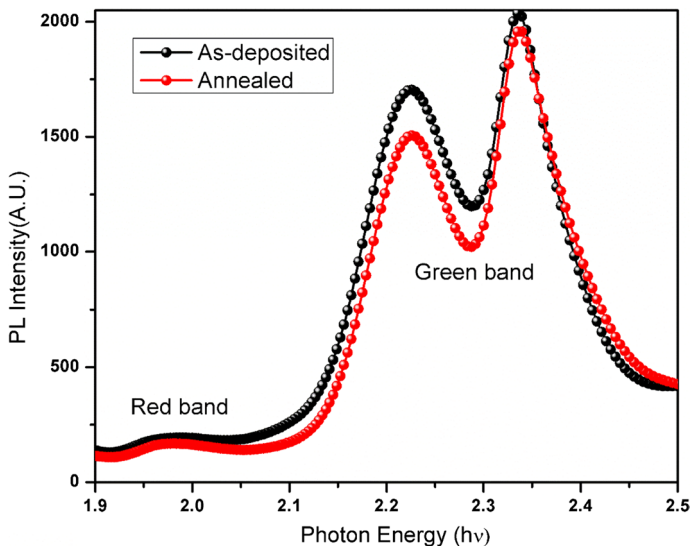


Fig. 7 Photoluminescence spectra of as-deposited and annealed CdS films

between the shallow donor Cd_i (cadmium interstitials) and VB. It is also mentioned in the literature, green band can be caused by the transition between the sulphur vacancies (Muthusamy and Muthukumar 2015; Narayanam et al. 2013; Meher et al. 2017). Vacancy and/or interstitials are commonly observed in as-grown films. However, density of such defects reduces after annealing which results in the reduction of intensity of corresponding bands (Meher et al. 2017).

3.5 Electrical characterization

3.5.1 Hall measurement

Under electrical characterization of semiconducting materials, Hall measurement is an inevitable study as it provides the important electrical parameters like resistivity, carrier density and mobility. In thin films, Hall effect measurement evolution is based on conformal mapping formulated by van der Pauw (Van der Pauw 1958). In the present case, measurements are carried out by considering uniformly deposited CdS thin films (5 mm × 5 mm) without isolated holes on it. As-deposited films have exhibited n-type conductivity with the resistivity of 6.69 Ω cm and carrier concentration $1.10 \times 10^{16} \text{ cm}^{-3}$ at room temperature. After annealing, films remained in n-type without significant change in the carrier concentration. However, the mobility has increased from 85 to 114 cm² V⁻¹ s⁻¹ with the slight decrease in the resistivity which may be due to the improved crystallinity and crystallite size occurred during the treatment as revealed in the XRD results. Canevari et al. obtained the n-type low resistivity CdS films by flash evaporation method and found the electron mobility in the range of 20–50 cm² V⁻¹ s⁻¹ (Canevari et al. 1984). Oboudi et al. have also observed the increase in mobility after annealing which is in accordance with present observation (Oboudi et al. 2013).

3.5.2 Temperature-dependent conductivity

Resistivity of as-grown and annealed CdS films was recorded over a temperature range of 20–300 K (Fig. 8). As observed from the graph, as-deposited films exhibited semiconducting behavior in 75–300 K temperature range and metallic behavior was observed below 75 K. Observed variation in resistivity with temperature has been explained by using percolation model (Christopher et al. 2016) which relates temperature with resistivity using following equation.

$$\rho(T) = \rho_0 + \rho_{1/2}T^{1/2} - \rho_s \ln T + \rho_5 T^5 + \rho_2 T^2 + \rho_{4.5} T^{4.5} \quad (4)$$

Scattering mechanism which mainly affects the transport properties can be analyzed through thermoelectric power (α) and resistivity (ρ) measurements. Fitting parameters are listed in Table 3. Literature review displays attempts made to explain transport properties in chalcogenide thin films (Jacome 2001; Jácome and Giraldo 2008). In case of polycrystalline materials, mostly resistive network model is used to explain the electric and thermoelectric properties. But percolation is a standard model for disordered systems. In polycrystalline films, grain boundaries are highly disordered, and they strongly affect the transport properties. In case of grain boundary transport, the electronic transport mechanism is dominated by random jumping motion of electrons along the grain boundary. Yilmaz and Faculty (2014) has studied the electrical conductivity of thermally evaporated CdS films in the temperature range 100–400 K and it demonstrated the change in the trend of resistivity

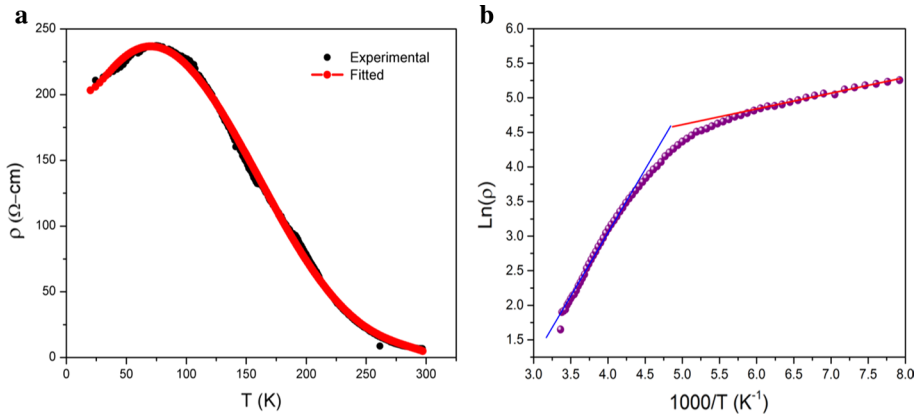


Fig. 8 **a** Variation of electrical resistivity with temperature for as-deposited CdS thin films. **b** Plot of $\text{Ln}(\rho)$ versus $1/T$ for as-deposited CdS thin films

Table 3 Resistivity measurement—fitting parameters

Parameter	Value
ρ_0 ($\Omega\text{-cm}$)	325.2
$\rho_{1/2}$ ($\Omega\text{-cm K}^{-1/2}$)	-84.45
ρ_s ($\Omega\text{-cm}$)	164
ρ_5 ($\Omega\text{-cm K}^{-5}$)	1.267×10^{-9}
ρ_2 ($\Omega\text{-cm K}^{-2}$)	0.02083
$\rho_{4.5}$ ($\Omega\text{-cm K}^{-4.5}$)	2.926×10^{-8}

near 100 K which is in line with our present report. However, the metallic type behaviour of the films has disappeared after annealing. This can be attributed the improved crystallinity/grain size of the film after annealing.

Electrical resistivity in the temperature range 125–300 K has been analyzed by Arrhenius equation (Hariech et al. 2012) to obtain thermal activation levels.

$$\rho = \rho_0 \exp\left(\frac{E_a}{kT}\right) \tag{5}$$

where E_a is the activation energy. The analysis has shown two distinct regions, 300–210 K and 210–125 K, corresponding to 0.148 and 0.016 eV respectively. These activation levels are generally attributed to disorder effect within the material (Hariech et al. 2012). S vacancy or Cd interstice are commonly observed donor defects in CdS films and slight excess of Cd observed in the present study supports it.

4 Conclusions

CdS thin films deposited by VE at room temperature favoured cubic structure. Even after annealing, the films remained in the cubic structure however it resulted in release

in strain. Raman study has shown four prominent bands and they are assigned to various modes. Shift in the peak position of various band in the annealed film may be attributed to strain release. Non-decomposition of the constituent elements of CdS has also been confirmed by the absence of band corresponding to sulphur in Raman spectra. Luminescence study showed emission in green and red region for both as-deposited and annealed films. Change in the intensity after annealing can be attributed to change in the surface to volume ratio. For annealed films, Hall measurement has shown increase in the mobility from 85 to 114 cm² V⁻¹ s⁻¹ without significant change in the carrier concentration and resistivity which can be attributed improved crystallinity. Low temperature electrical conductivity study has shown semiconducting behaviour of the film till 75 K. Below 75 K, film exhibited metallic behaviour and the electrical transport has been explained by percolation model which is appropriate to describe the grain boundary transport in polycrystalline thin films.

Acknowledgements The authors are grateful to VGST, Govt. of Karnataka State India (VGST/K-FIST(L1)/GRD-377/2014-15) for financial assistance.

References

- Abdulkhadar, M., Thomas, B.: Study of Raman spectra of nanoparticles of CdS and ZnS. *Nanostruct. Mater.* **5**, 289–298 (1995)
- Badr, Y., Abd El-Kader, K., Khafagy, R.: Raman spectroscopic study of CdS, PVA composite films. *J. Appl. Polym. Sci.* **92**, 1984–1992 (2004)
- Boakye, F., Nusenu, D.: The energy band gap of cadmium sulphide. *Solid State Commun.* **102**, 323–326 (1997)
- Britt, J., Ferekides, C.: Thin-film CdS/CdTe solar cell with 15.8% efficiency. *Appl. Phys. Lett.* **62**, 2851–2852 (1993)
- Canevari, L.Z., Romeo, V.N., Sberveglieri, G., Azzi, S., Tosi, A., Curti, M.: Low resistivity CdS thin films grown by flash-evaporation at low substrate temperature. *J. Vac. Sci. Technol. A Vac. Surf. Films* **2**, 9–10 (1984)
- Chandramohan, S., Sathyamoorthy, R., Sudhagar, P., Kanjilal, D., Kabiraj, D., Asokan, K., Ganesan, V., Shripathi, T., Deshpande, U.: High-energy heavy-ion induced physical and surface-chemical modifications in polycrystalline cadmium sulfide thin films. *Appl. Phys. A* **94**, 703–714 (2008)
- Chi, T.T.K., Gouadec, G., Colomban, P., Wang, G., Mazerolles, L., Liem, N.Q.: Off-resonance Raman analysis of wurtzite CdS ground to the nanoscale: structural and size-related effects. *J. Raman Spectrosc.* **42**, 1007–1015 (2011)
- Christopher, B., Rao, A., Petwal, V., Verma, V., Dwivedi, J., Lin, W., Kuo, Y.: Influence of electron beam irradiation on electrical, structural, magnetic and thermal properties of Pr 0.8 Sr 0.2 MnO 3 manganites. *Physica B* **502**, 119–131 (2016)
- Chu, T., Chu, S., Britt, J., Ferekides, C., Wang, C., Wu, C., Ullal, H.: 14.6% efficient thin-film cadmium telluride heterojunction solar cells. *IEEE Electron. Dev. Lett.* **13**, 303–304 (1992)
- Chuu, D.S., Dai, C.M., Hsieh, W.F., Tsai, C.T.: Raman investigations of the surface modes of the crystallites in CdS thin films grown by pulsed laser and thermal evaporation. *J. Appl. Phys.* **69**, 8402–8404 (1991)
- Dzhagan, V., Milekhin, A.G., Valakh, M.Ya., Pedetti, S., Tessier, M., Dubertrete, B., Zahna, D.R.T.: Morphology-induced phonon spectra of CdSe/CdS nanoplatelets: core/shell vs. core-crown. *Nanoscale* **8**, 17204–17212 (2016)
- El Assali, K., Boustani, M., Khiara, A., Bekkay, T., Outzourhit, A., Ameziane, E., Bernede, J., Pouzet, J.: Some structural and optical properties of CdS thin films prepared by RF sputtering. *Phys. Status Solidi (a)* **178**, 701–708 (2000)
- Farid, S., Stroschio, M.A., Dutta, M.: Raman scattering investigations of CdS thin films grown by thermal evaporation. *AIP Conf. Proc.* **45**, 45–48 (2012)
- Filippidis, L., Siegle, H., Hoffmann, A., Thomsen, C.: Hyper-Raman scattering on GaN and CdS. *Phys. Status Solidi (B)* **212**, R1–R2 (1999)
- Hariech, S., Aida, M., Moualkia, H.: Observation of Meyer–Neldel rule in CdS thin films. *Mater. Sci. Semicond. Process.* **15**, 181–186 (2012)

- Hasnat, A., Podder, J.: Effect of annealing temperature on structural, optical and electrical properties of pure CdS thin films deposited by spray pyrolysis technique. *Adv. Mater. Phys. Chem.* **02**, 226–231 (2012)
- Hwang, J.Y., Monteiro, S.N., Bai, C.G., Carpenter, J., Cai, M., Firrao, D., Kim, B.G.: *Characterization of Minerals, Metals, and Materials*, pp. 251–258. Wiley (2012)
- Irimpan, L., Ambika, D., Kumar, V., Nampoore, V.P.N., Radhakrishnan, P.: Effect of annealing on the spectral and nonlinear optical characteristics of thin films of nano-ZnO. *J. Appl. Phys.* **104**, 33118-1–33118-9 (2008)
- Jacome, C.: Study of electrical transport properties in polycrystalline CdTe thin films. *Thin Solid Films* **396**, 257–263 (2001)
- Jácome, C., Giraldo, J.: Properties of ZnO thin films through percolation model. *Microelectron. J.* **39**, 1316–1317 (2008)
- Kozytskiy, A.V., et al.: Photoelectrochemical and Raman characterization of nanocrystalline CdS grown on ZnO by successive ionic layer adsorption and reaction method. *Thin Solid Films* **562**, 56–62 (2014)
- Lee, J.: Raman scattering and photoluminescence analysis of B-doped CdS thin films. *Thin Solid Films* **451–452**, 170–174 (2004)
- Leite, R.C.C., Scott, J.F., Damen, T.C.: Multiple-phonon resonant raman scattering in CdS. *Phys. Rev. Lett.* **22**, 780–782 (1969)
- Meher, S., Kaushik, D., Subrahmanyam, A.: Native defects in sol–gel derived CdS buffer layers for photo-voltaic applications. *J. Mater. Sci. Mater. Electron.* **28**, 6033–6046 (2017)
- Muthusamy, M., Muthukumaran, S.: Effect of Cu-doping on structural, optical and photoluminescence properties of CdS thin films. *Optik* **126**, 5200–5206 (2015)
- Nanda, K.K., Sarangi, S.N., Sahu, S.N., Deb, S.K., Behera, S.N.: Raman spectroscopy of CdS nanocrystalline semiconductors. *Physica B* **262**, 31–39 (1999)
- Narayanam, P.K., Soni, P., Mohanta, P., Srinivasa, R.S., Talwar, S.S., Major, S.S.: Effect of heat treatment on the photoluminescence of CdS nanocrystallites in cadmium-rich organic Langmuir Blodgett matrix. *Mater. Chem. Phys.* **139**, 196–209 (2013)
- Oboudi, S.F., Mohamed, G.H., Khalaf, K., Adem, K.A.: Synthesis and study of annealing effect on electrical properties of CdS doped Zn thin films. *Int. J. Thin Films Sci. Technol.* **275**, 267–275 (2013)
- Oliva, A., Castro-Rodríguez, R., Soñis-Canto, O., Sosa, V., Quintana, P., Peña, J.: Comparison of properties of CdS thin films grown by two techniques. *Appl. Surf. Sci.* **205**, 56–64 (2003)
- Prabhar, S., Dhanam, M.: CdS thin films from two different chemical baths—structural and optical analysis. *J. Cryst. Growth* **285**, 41–48 (2005)
- Qinghui, Y., Huaiwu, Z., Yingli, L.I.U., Qiye, W.E.N.: Magneto-optical properties of nanometer scale Bi:YIG films. *J. Chin. Ceram. Soc.* **35**, 1190–1193 (2007)
- Sakai, H., Tamaru, T., Sumomogi, T., Ezumi, H., Ullrich, B.: Crystal direction of CdS thin film produced by laser ablation. *Jpn. J. Appl. Phys.* **37**, 4149–4153 (1998)
- Senthil, G.L.N.R., Mangalaraj, K.D., Narayandass, S.K., Kesavmoorthy, R.: Raman scattering and XRD analysis in argon ion implanted CdS thin films prepared by vacuum evaporation. *Nucl. Instrum. Methods Phys. Res. B* **173**, 475–482 (2001)
- Sivasubramanian, V., Arora, A.K., Premila, M., Sundar, C.S., Sastry, V.S.: Optical properties of CdS nanoparticles upon annealing. *Physica E* **31**, 93–98 (2006)
- Tell, B., Damen, T., Porto, S.: Raman effect in cadmium sulfide. *Phys. Rev.* **144**, 771–774 (1966)
- Trajić, J., et al.: Raman spectroscopy of optical properties in CdS thin films. *Sci. Sinter.* **47**, 145–152 (2015)
- Ullrich, B., Tomm, J., Dushkina, N., Tomm, Y., Sakai, H., Segawa, Y.: Photoelectric dichroism of oriented thin film CdS fabricated by pulsed-laser deposition. *Solid State Commun.* **116**, 33–35 (2000)
- Van der Pauw, L.J.: A method of measuring the resistivity and hall coefficient on lamellae of arbitrary shape. *Philips Tech. Rev.* **20**, 220–224 (1958)
- Von Dreele, R., Jorgensen, J., Windsor, C.: Rietveld refinement with spallation neutron powder diffraction data. *J. Appl. Crystallogr.* **15**, 581–589 (1982)
- Wu, X., Dhere, R.G., Albin, D.S., Gessert, T.A., Dehart, C., Keane, T.C., Duda, A., Coutts, T.J., Asher, S., Levi, D.H., Moutinho, H.R., Yan, Y., Moriarty, T., Johnson, S., Emery, K., Sheldon, P.: High Efficiency CTO/ZTO/CdS/CdTe Polycrystalline Thin-Film Solar Cells. National Center for Photovoltaics Program Review Meeting, Lakewood, CO. No. cp-250-31025 (2001)
- Yilmaz, K., Faculty, A.: Some structural, electrical and optical properties of vacuum evaporated CdS thin films. *J. Ovonic Res.* **10**, 211–219 (2014)